

A THEORY OF RADIATION-INDUCED SEGREGATION IN CONCENTRATED ALLOYS *

H. WIEDERSICH, P.R. OKAMOTO and N.Q. LAM

Materials Science Division, Argonne National Laboratory, Argonne, IL 60439, USA

Received 1 March 1979

A new and simple theory for radiation-induced segregation in concentrated alloys is presented. The coupling between defect fluxes and atom fluxes is accounted for by the concept of preferential migration of vacancies and interstitials via A-atoms or B-atoms in a binary A–B alloy. Similarly, atom fluxes are partitioned into those occurring via vacancies and via interstitials. This approach permits expression of the defect fluxes and atom fluxes in terms of partial diffusivity coefficients and concentration gradients of defects and alloy components. The time and space dependence of the defect concentrations and composition of a binary alloy is described by a set of three coupled partial differential equations containing four partial diffusivity coefficients, i.e., those of A-atoms and B-atoms diffusing via vacancies and via interstitials. The set of differential equations has been integrated for some model binary alloys with complete miscibility, utilizing the geometry of a thin foil. The sample calculations are in good qualitative agreement with the general features of radiation-induced segregation as deduced from experiments. The temperature, dose and dose-rate dependencies of segregation in concentrated alloys are found to be similar to those predicted by the Johnson–Lam model for dilute alloys.

1. Introduction

In the past few years, considerable evidence has been found for spatial redistribution of alloy components on a microscopic scale during high-temperature irradiations. Several recent reviews [1–4] summarize the experimental evidence and describe theoretical models of the phenomenon. Extensive references to the original work are given in these papers. This radiation-induced segregation phenomenon can lead to enrichment or depletion of alloying elements in regions near surfaces, dislocations, voids, grain boundaries, and boundaries between phases. The local compositional change may be of sufficient severity to cause precipitation of a phase not present in the homogeneous alloy after thermal ageing at the same temperatures. Conversely, local changes in composition near precipitate interfaces may cause the dissolution of precipitates.

The radiation-induced segregation phenomenon has its origin in the coupling between defect fluxes and fluxes of alloying elements. Energetic irradiation produces point defects and defect clusters with an

approximately random distribution throughout the material. Those defects that are mobile and escape recombination are reincorporated into the crystal structure at dislocations, grain boundaries and other defect sinks. Hence, irradiation induces defect fluxes from the interior of the grains to spatially discrete sinks. Since the motion of defects is caused by the motion of atoms, fluxes of atoms are associated with defect fluxes. Any preferential association of defects with a particular alloying component and/or preferential participation of a component in defect diffusion will couple a net flux of the alloying element to the defect fluxes. The flux of an element causes a buildup or depletion of alloying elements in the vicinity of defect sinks and, therefore, concentration gradients in initially homogeneous alloy phases. The concentration gradients induce back diffusion of the segregating elements, and a quasi-steady state may be set up during irradiation whenever the defect-driven alloying-element fluxes are balanced by the back diffusion.

Whereas extensive theoretical modeling of segregation in dilute alloys has been performed, mainly by Johnson and Lam [2], the extension to concentrated alloys has been limited to some unpublished work by

* Work supported by the US Department of Energy.

Manning [5] and a similar, more recent treatment by Marwick [6]. The latter treatment is restricted to the effects of the vacancy flow, i.e., the inverse Kirkendall effect, and is likely to be of limited use because there exist copious experimental indications of the importance of solute coupling to interstitial fluxes. In the following we will develop a new and simple treatment of radiation-induced segregation in concentrated alloys. The model retains all the important physical features required to give a realistic description of the phenomenon with a minimum set of physical parameters which, at least for vacancies, are experimentally accessible.

2. Basic model

2.1. General kinetic equations

We will consider a binary solid solution of the elements A and B, and we will assume throughout that the two species are distributed randomly on a local scale, i.e., no short- or long-range order exists. As a consequence of irradiation, the local concentrations of vacancies C_v and of interstitials C_i change with time t according to

$$\frac{\partial C_v}{\partial t} = -\nabla J_v + K_0 - R \quad (1a)$$

and

$$\frac{\partial C_i}{\partial t} = -\nabla J_i + K_0 - R, \quad (1b)$$

where $-\nabla J_v$ and $-\nabla J_i$ are the divergencies of the fluxes J of vacancies and interstitials, respectively, K_0 is the production rate of vacancies and interstitials by irradiation, and R is the rate of recombination of vacancies and interstitials. In any local region that does not contain a defect sink, the rates K_0 and R for interstitials are, by necessity, equal to those for vacancies. (We assume here for simplicity that defect clusters produced in cascades either decompose thermally or are annihilated by the opposite type of defect; these defects are included in K_0 and R , respectively.) The conservation equations for the alloying elements A and B are

$$\frac{\partial C_A}{\partial t} = -\nabla J_A \quad (2a)$$

and

$$\frac{\partial C_B}{\partial t} = -\nabla J_B. \quad (2b)$$

The right-hand sides (RHS) of eqs. (2a) and (2b) contain only the divergencies of the atom fluxes. (For the case of self-ion bombardment one could add an appropriate term to these equations in the end-of-range region.) The defect and atom fluxes in eqs. (1) and (2) arise from forces due to chemical potential gradients. For simplicity, we will use here relations between fluxes and concentration gradients. The coupling between atom and defect fluxes is based on simple physical models instead of the formalism of the phenomenological equations.

The assumption is made that diffusive motions of A- and B-atoms occur only by vacancy and by interstitialcy or interstitial jumps. The strongest and by far the most important coupling between atom and defect fluxes in the present context arises from the necessity that a flux of interstitials drives a flux of A- and B-atoms equal in size and direction to that of the interstitials across any fixed "lattice" or "marker" plane:

$$J_i = J_A^i + J_B^i \quad (3)$$

and, similarly, that a flux of vacancies drives a flux of A- and B-atoms equal in size, but opposite in direction, across the marker plane:

$$J_v = -(J_A^v + J_B^v). \quad (4)$$

In eqs. (3) and (4) and subsequently, the subscripts indicate the species of flux considered, and the superscripts the complementary species via which the flux occurs. In general, the division of the interstitial and vacancy fluxes via A- and B-atoms will not be in the same proportion as the atom fractions N_A and N_B , e.g., vacancies may migrate preferentially via B-atoms and interstitials preferentially via A-atoms.

2.2. Partial diffusion coefficients

In order to express the fluxes of atoms and defects in terms of the gradients of the different species, we will define partial diffusion coefficients in the following way:

$$D_A^v = \frac{1}{6} b_v^2 z_v N_v \nu_A^v f_A^v, \quad (5)$$

e.g., the partial diffusion coefficient of A-atoms via vacancies is proportional to the jump frequency ν_A^v with which an A-atom exchanges with a vacancy on a given neighboring site. N_v is the atomic fraction of vacancies; the quantity $z_v N_v$ is the probability that one of the z_v neighboring sites to the A-atom is occupied by a vacancy; b_v is the jump distance; and f_A^v is the correlation factor for A-atoms migrating by vacancies, which takes into account the greater than random probability that after an initial jump, subsequent jumps of the A-atom will have a displacement component opposite to that of the initial jump. In cubic crystals of a single element, the correlation factor f varies from 0.5 in the diamond structure to 0.78146 in the face-centered-cubic structure [7]. In alloys, f depends in a complicated way on the various different vacancy jump frequencies and on the composition [7,8]. However, values of the correlation factors in concentrated alloys are expected to deviate only moderately from unity except in pathological cases. Since a number of physical quantities necessary to describe radiation-induced segregation are not very precisely known, we will neglect correlation factors for the sake of simplicity. Thus, eq. (5) becomes

$$D_A^v = \frac{1}{6} b_v^2 z_v N_v \nu_A^v . \quad (6)$$

Correspondingly, we can write the partial diffusion coefficients for vacancies via A-atoms as

$$D_v^A = \frac{1}{6} b_v^2 z_v N_A \nu_v^A . \quad (7)$$

Note that $\nu_v^A = \nu_A^v$ ($\equiv \nu_{Av}$) since either jump frequency involves the exchange of a given A-atom-vacancy pair.

Thus far we have assumed that the vacancies are randomly distributed in the alloy. If a preferential association between vacancies and A-atoms (or B-atoms) existed, we could incorporate it in a crude fashion into eqs. (6) and (7) by a Boltzmann factor involving a binding energy. To avoid undue proliferation of the number of physical parameters required to evaluate the model, we will incorporate such a factor into the exchange frequency, making it an "effective" jump frequency.

For convenience, we combine those factors on the RHS of eqs. (6) and (7) that are common to both,

$$d_{Av} = \frac{1}{6} b_v^2 z_v \nu_{Av} , \quad (8)$$

so that the partial diffusion coefficients take the form

$$D_a^v = d_{Av} N_v \quad (9)$$

and

$$D_v^A = d_{Av} N_A . \quad (10)$$

The partial diffusion coefficients for B-atoms via vacancies and vacancies via B-atoms are, respectively,

$$D_B^v = d_{Bv} N_v \quad (11)$$

and

$$D_v^B = d_{Bv} N_B , \quad (12)$$

with

$$d_{Bv} = \frac{1}{6} b_v^2 z_v \nu_{Bv} , \quad (13)$$

where ν_{Bv} is the effective exchange-jump frequency of a B-atom-vacancy pair which includes a factor accounting for possible binding or repulsion between vacancies and B-atoms. We note that the two quantities d_{Av} and d_{Bv} , which will be called diffusivity coefficients, can be obtained from tracer-diffusion or interdiffusion experiments that include the measurement of the Kirkendall effect and from measurements of the thermal equilibrium concentration of vacancies in the alloy.

The partial diffusion coefficients of the elements via interstitials, and of interstitials via A- and B-atoms, are easily derived and are of the same form as the quantities given for vacancies in eqs. (8) to (13) with the sub- and superscripts v replaced by i, provided the migration occurs by an interstitial mechanism. For example, the diffusion coefficient of A-atoms via interstitials is

$$D_A^i = \frac{1}{6} b_i^2 z_i \nu_A^i N_A^i / N_A , \quad (14)$$

where b_i is the jump distance to a nearest-neighbor interstitial site, z_i is the interstitial-site coordination number, ν_A^i is the jump frequency of an A-atom interstitial to a given nearest-neighbor interstitial site and N_A^i / N_A is the fraction of A-atoms that are in interstitial sites. For random occupation of interstitials by A- and B-atoms, $N_A^i = N_i N_A$, and we obtain

$$D_A^i = \frac{1}{6} b_i^2 z_i N_i \nu_A^i , \quad (15)$$

which is entirely analogous to the partial diffusion coefficient of A-atoms via vacancies, eq. (6).

However, the details of the situation become considerably more complex when interstitials migrate via

an interstitialcy mechanism, because more than one atom is significantly involved in any interstitialcy jump. Nevertheless, we will assume the validity of the concept that interstitials migrate via A-atoms or B-atoms, and that the partial diffusion coefficients can be written in the same form as those for vacancies, eqs. (9) to (12); thus,

$$D_A^i = d_{Ai}N_i, \quad (16)$$

$$D_i^A = d_{Ai}N_A, \quad (17)$$

$$D_B^i = d_{Bi}N_i, \quad (18)$$

and

$$D_i^B = d_{Bi}N_B. \quad (19)$$

The expression for d_{Ai} and d_{Bi} will depend on the details of the interstitialcy mechanism and will be more complicated than eqs. (8) and (13).

The advantage of writing the partial diffusion coefficients in the form $D = dN$ arises from the fact that the major compositional and, therefore, spatial dependence resides in the factor N , whereas d contains the kinetic and diffusional information for the atom-vacancy or atom-interstitial complexes. The values of d depend to a degree on the composition and, therefore, on spatial coordinates, via the jump frequencies and preferential association of defects with atoms of one or the other component. However, to a first approximation it is reasonable to assume that the d 's are composition-independent unless experimental information to the contrary is available.

From eqs. (9) to (12) and (16) to (19) we may define "average" or "total" diffusion coefficients for the various species:

$$D_v = d_{Av}N_A + d_{Bv}N_B, \quad (20)$$

$$D_i = d_{Ai}N_A + d_{Bi}N_B, \quad (21)$$

$$D_A = d_{Av}N_v + d_{Ai}N_i, \quad (22)$$

and

$$D_B = d_{Bv}N_v + d_{Bi}N_i. \quad (23)$$

2.3. Flux and diffusion equations

With the aid of the partial and total diffusion coefficients we can now write down the fluxes of atoms and defects with respect to a coordinate sys-

tem fixed on the crystal lattice:

$$J_A = -D_A\alpha\nabla C_A + d_{Av}N_A\nabla C_v - d_{Ai}N_A\nabla C_i, \quad (24)$$

$$J_B = -D_B\alpha\nabla C_B + d_{Bv}N_B\nabla C_v - d_{Bi}N_B\nabla C_i, \quad (25)$$

$$J_v = d_{Av}N_v\alpha\nabla C_A + d_{Bv}N_v\alpha\nabla C_B - D_v\nabla C_v \\ = (d_{Av} - d_{Bv})N_v\alpha\nabla C_A - D_v\nabla C_v, \quad (26)$$

and

$$J_i = -d_{Ai}N_i\alpha\nabla C_A - d_{Bi}N_i\alpha\nabla C_B - D_i\nabla C_i \\ = -(d_{Ai} - d_{Bi})N_i\alpha\nabla C_A - D_i\nabla C_i. \quad (27)$$

The thermodynamic factor $\alpha = (1 + \partial \ln \gamma_A / \partial \ln N_A) = (1 + \partial \ln \gamma_B / \partial \ln N_B)$ takes care of the difference between the chemical potential gradient, which is the true driving force for the diffusion of A- and B-atoms, and the concentration gradient. γ_A and γ_B are the activity coefficients. The thermodynamic factor deviates from unity for nonideal solutions and can be derived for some alloy systems from available thermodynamic data. We have not included a corresponding factor in the defect-gradient terms, since no values for defect-activity coefficients are available. The first terms on the RHS of eqs. (24) and (25) are the atom fluxes induced by the chemical-composition gradient; the second and third terms are the atom fluxes driven by the vacancy and interstitial gradients, respectively. The defect fluxes represented by the near-RHS of eqs. (26) and (27) are driven by the A- and B-atom concentration gradients and by their own gradients, respectively. The far-RHS of eqs. (26) and (27) are obtained by neglecting the small perturbations arising from the presence of the defects, so that $\nabla C_B = -\nabla C_A$. The first terms on the far-RHS of eqs. (26) and (27) are the Kirkendall effects from the vacancy and the interstitial diffusion mechanisms, respectively; i.e., the difference in the A- and B-atom fluxes in opposite direction past a marker plane must be made up by an appropriate defect flux. Of the four flux equations, eqs. (24) to (27), only three are independent because atom fluxes and defect fluxes through a marker plane must balance:

$$J_A + J_B = -J_v + J_i. \quad (28)$$

The minus sign in front of the vacancy flux derives from the fact that vacancies move in the opposite direction to the atoms.

To obtain the evolution of atom and defect distri-

butions in time and space, the set of coupled partial differential equations given earlier [eqs. (1) and (2)] must be solved for appropriate initial and boundary conditions. Inserting the fluxes given by eqs. (24) to (27) into eqs. (1) and (2), we obtain

$$\frac{\partial C_v}{\partial t} = \nabla[-(d_{Av} - d_{Bv})\alpha\Omega C_v \nabla C_A + D_v \nabla C_v] + K_0 - R,$$

$$\frac{\partial C_i}{\partial t} = \nabla[(d_{Ai} - d_{Bi})\alpha\Omega C_i \nabla C_A + D_i \nabla C_i] + K_0 - R, \quad (29)$$

and

$$\frac{\partial C_A}{\partial t} = \nabla[D_A \alpha \nabla C_A + \Omega C_A (d_{Ai} \nabla C_i - d_{Av} \nabla C_v)].$$

Here the atomic fractions N have been converted into volume concentrations according to the relationship $N = \Omega C$, where Ω is the average atomic volume of the alloy. Also, we have omitted the equation for the element B because it is not independent and $C_B = 1 - C_A$ when the small defect concentrations are neglected. We note that, even in the conceptually simplest case where the diffusivity coefficients d are independent of the concentration, terms of the form $\nabla C_v \cdot \nabla C_A$ and $\nabla C_i \cdot \nabla C_A$ are present in eq. (29).

2.4. Steady-state segregation

Some qualitative conclusions can easily be derived from the flux equations, eqs. (24)–(27), by assuming steady state has been achieved. At steady state,

$$J_A = J_B = 0, \quad (30)$$

and neglecting bias effects, e.g., preferential absorption of interstitials on dislocations,

$$J_v = J_i. \quad (31)$$

The latter equation must hold because equal numbers of interstitials and vacancies are produced by irradiation, equal numbers are lost by recombination and, hence, equal numbers of interstitials and vacancies must migrate to sinks at steady state. One can eliminate ∇C_i in eq. (24) with the aid of eqs. (31), (26) and (27), and derive the following relation between ∇C_A and ∇C_v from $J_A = 0$ [eq. (30)]:

$$\nabla C_A = \frac{N_A N_B d_{Bi} d_{Ai}}{\alpha (d_{Bi} N_B D_A + d_{Ai} N_A D_B)}$$

$$\times \left(\frac{d_{Av}}{d_{Bv}} - \frac{d_{Ai}}{d_{Bi}} \right) \nabla C_v. \quad (32)$$

From eq. (32) it is evident that the relation between the direction of the gradient of alloy component A and that of the vacancy gradient is determined by the relative magnitude of the ratios d_{Av}/d_{Bv} and d_{Ai}/d_{Bi} , which are essentially the ratios of the “effective” jump frequencies of A- and B-atoms into neighboring vacancies and of A- and B-interstitials, respectively. These jump frequencies may contain terms accounting for preferential association of interstitials and/or vacancies with A or B atoms as discussed in the paragraph below eq. (7). During irradiation, the vacancy concentration always decreases towards a defect sink, and eq. (32) predicts that the element A becomes enriched at sinks if $d_{Ai}/d_{Bi} > d_{Av}/d_{Bv}$, i.e., if preferential transport of A-atoms via interstitials outweighs preferential transport via vacancies and vice versa.

2.5. Applicability and limitations of the model

Before the results of sample calculations are discussed in the next section, some comments on the applicability and limitations of the simple model developed here will be made. We have abandoned the concept of distinct complexes of A- or B-atoms with vacancies. The concept of bound defect-solute complexes which migrate as entities has been used successfully in the model describing segregation in dilute alloys [2]. However, as the concentration of substitutional solute is increased above a few percent, one has to include defect-solute complexes containing more than one solute atom. This increases not only the complexity of the model but also the number of unknown physical parameters such as binding and migration energies of the higher-order complexes. At somewhat higher solute concentrations, the concept of migrating vacancy-solute complexes becomes ill-defined because most of the time, a vacancy will have as nearest neighbors several solute atoms which are likely to change identity as the vacancy migrates. The elimination of migrating vacancy-solute complexes from the present model excludes its application to those dilute alloys in which solute transport by tightly bound vacancy-solute pairs is important.

The situation with regard to interstitial complexes

is somewhat different in nature. There is ample indication, both experimental [1,3,4] and theoretical [9], that undersized solutes form tightly bound solute-interstitial complexes. Furthermore, it seems likely that these complexes migrate as solute interstitials. (The combined in-place rotation of the mixed dumbbell and cage motion of the undersized solute suggested by Dederichs et al. [9] for the long-range diffusion of the tightly bound mixed dumbbell is in effect a solute–interstitial migration.) Thus, the present model for segregation appears well suited to describe alloy systems with significant atomic size differences, including the limit in which the undersized component is present in dilute solution. However, it is important to include in the diffusivity coefficients D_A^i and D_B^i factors which represent the non-random occupation of interstitials by A- and B-atoms, respectively. The fractions of A- and B-interstitials can be adequately represented by

$$N_A^i = N_i \frac{N_A \exp(H_{Ai}^b/kT)}{N_A \exp(H_{Ai}^b/kT) + N_B}, \quad (33)$$

and

$$N_B^i = N_i \frac{N_B}{N_A \exp(H_{Ai}^b/kT) + N_B}, \quad (34)$$

where H_{Ai}^b is the energy gained by converting a B-interstitial into an A-interstitial, k is the Boltzmann constant, and T is the absolute temperature.

The application of the present model to alloy systems with a size mismatch insufficient to convert the interstitialcy-type migration (which is the generally accepted mechanism in pure metals) to a predominantly interstitial migration, via the undersized-component interstitials, appears somewhat questionable. The simplification used in the model (i.e., interstitialcy migration is assumed to occur only via A- or B-atoms, and interstitialcy jumps simultaneously involving A- and B-atoms are neglected) is not believed to seriously impair the applicability of the model to concentrated alloys with interstitialcy migration. If interstitialcies migrate significantly faster via one component in a concentrated alloy, jumps involving both components will be infrequent and will affect the segregation process only insignificantly. On the other hand, if interstitialcies migrate with equal ease via either component, jumps involving both types of atoms will be frequent but the con-

tribution of the interstitials to segregation will be insignificant.

3. Sample calculations

Numerical solutions of the system of partial differential equations, eq. (29), were obtained for a thin foil by means of the GEAR package of subroutines [10], starting from the thermodynamic equilibrium conditions. The foil, of thickness $L = 500$ nm, was assumed to be free of internal sinks so that segregation could occur only to the surfaces. The calculations were performed for only half of the foil because of the symmetry of the problem. Conditions at the boundaries, i.e. at the surface and at the foil center, were defined as follows. At the foil center ($x = \frac{1}{2}L$), all concentration gradients were set equal to zero:

$$\frac{\partial C_i(t, \frac{1}{2}L)}{\partial t} = \frac{\partial C_v(t, \frac{1}{2}L)}{\partial x} = \frac{\partial C_A(t, \frac{1}{2}L)}{\partial x} = 0, \quad (35)$$

whereas at the foil surface ($x = 0$), the concentrations of interstitials and vacancies were fixed at their thermal equilibrium values,

$$C_i(t, 0) = \exp(-H_i^f/kT),$$

and

$$C_v(t, 0) = \exp(S_v^f/k) \exp(-H_v^f/kT), \quad (36)$$

where H_i^f and H_v^f are the effective formation energies of interstitials and vacancies in the alloy (taken here as 4.0 and 1.6 eV, respectively) and S_v^f is the effective entropy for vacancy formation ($= 3k$). The missing boundary condition at the foil surface, i.e., the concentration of element A, was replaced by the conservation condition

$$\int_0^{L/2} C_A(t, x) dx = \frac{1}{2} C_A^0 L, \quad (37)$$

where C_A^0 is the initially uniform concentration of A. A spatially uniform defect production rate K_0 was used in all sample calculations.

We will discuss some results for model alloy systems with complete miscibility. The formation energies and pre-exponentials for vacancies and interstitials are taken to be similar to those of pure nickel and are assumed to be independent of composition.

3.1. Segregation by preferential defect migration

For the first example, the pre-exponentials and the migration energies of vacancies (H_{Av}^m, H_{Bv}^m) and of interstitials (H_{Ai}^m, H_{Bi}^m) via A- and B-atoms are assumed similar to those for pure copper (A) and for pure nickel (B), respectively, and are also taken to be independent of composition. Association of defects with A- and B-atoms is assumed to be nonpreferential. The concentration profiles which develop at 500°C are shown in fig. 1 for the near-surface region at several times after the start of irradiation. Strong depletion of the A component near the surface is apparent. This result is expected from eq. (32) because

$$d_{Av}/d_{Bv} \{= \exp[(H_{Bv}^m - H_{Av}^m)/kT]\}$$

$$\gg d_{Ai}/d_{Bi} \{= \exp[H_{Bi}^m - H_{Ai}^m/kT]\};$$

i.e. the preferential transport of A-atoms away from the surface by vacancies for outweighs their preferential transport towards the surface by interstitials. The depletion commences quickly near the surface. As the time (or dose) increases, the concentration gradient becomes less steep and depletion of A extends deeper into the foil, approaching steady state by $\sim 10^4$ s (or ~ 10 dpa). Note that the concentration of A is severely reduced (from 25 to 0.15 at%) at the surface, whereas the increase in the center of the foil (not shown in fig. 1) is less significant (to 26.5 at%).

Steady-state profiles calculated for the same set of parameters as used for fig. 1 are shown for several irradiation temperatures in fig. 2. The concentration profiles are steep and shallow in depth at low temper-

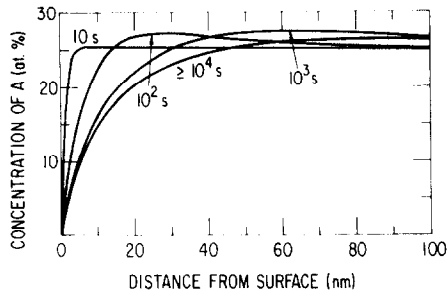


Fig. 1. Concentration of component A as a function of depth for several irradiation times. B-25 at% A alloy, foil thickness 500 nm, displacement rate 10^{-3} dpa/s, $H_{Av}^m = 0.77$ eV, $H_{Bv}^m = 1.28$ eV, $H_{Ai}^m = 0.1$ eV, $H_{Bi}^m = 0.15$ eV, temperature 500°C.

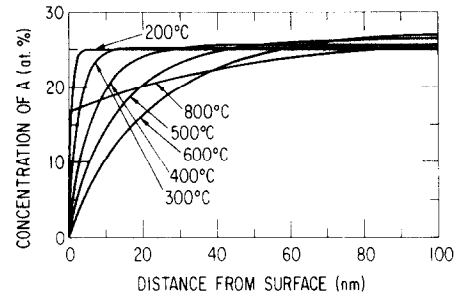


Fig. 2. Steady-state concentration of component A as a function of depth for several irradiation temperatures. Parameters are the same as for fig. 1.

atures; they become less steep and extend further into the foil at increasingly higher temperatures. The amount of segregation, characterized either by the surface concentration or by the amount of component A transported to the interior from the near surface region where $C_A < C_A^0$ goes through an extremum as a function of temperature. This illustrated in the lower portion of fig. 3, which shows that steady-state surface concentration as a function of irradiation temperature for two different dose rates. The general shape of the curves is easily understood qualitatively. At high temperatures, a large thermal vacancy concentration leads to a high diffusion rate of alloying elements as well as to a high defect-recombination

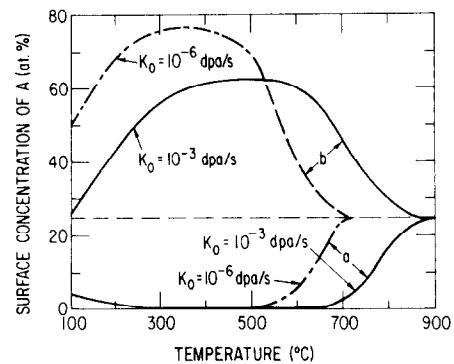


Fig. 3. Steady-state surface concentration of component A as a function of irradiation temperature for two displacement rates K_0 . Common parameters: B-25 at% A alloy, foil thickness 500 nm, $H_{Bv}^m = 1.28$ eV, $H_{Av}^m = 0.1$ eV, $H_{Bi}^m = 0.15$ eV. Bottom: $H_{Av}^m = 0.77$ eV; predominant transport of A by vacancies leads to surface depletion of A. Top: $H_{Av}^m = H_{Bv}^m = 1.28$ eV; predominant transport of A by interstitials with $H_{Ai}^m < H_{Bi}^m$ leads to surface enrichment.

rate; the latter reduces the defect fluxes to sinks and hence the cause of segregation, while the former increases the back diffusion of segregated alloying elements. At intermediate temperatures, the thermal vacancy concentration becomes insignificant and the radiation-induced excess vacancy concentration is relatively low; because the vacancy mobility is high, the defect recombination rate is low, and hence defects migrate predominantly to sinks and significant segregation occurs. At low temperatures, the vacancy mobility is low, the radiation-induced excess vacancy concentration is correspondingly high, defect recombination becomes dominant, and hence the defect fluxes to sinks decrease and segregation is reduced. The shift of the curve for the lower displacement rate toward lower temperatures is related to the fact that more time is available at the low dose rate, and the individual thermally activated rate processes involved in the segregation process can proceed at lower speed with similar results.

If the energy for migration of vacancies via A-atoms is set equal to that via B-atoms, i.e. no preferential transport occurs via vacancy fluxes, enrichment of component A occurs at the surface because now $d_{Av}/d_{Bv} < d_{Ai}/d_{Bi}$. This is illustrated in the upper part of fig. 3, which shows the steady-state surface concentration as a function of temperature calculated for the same set of physical parameters as for the lower part of fig. 3, except $H_{Av}^m = H_{Bv}^m = 1.28$ eV. In this case, the preferential migration of interstitials via A-atoms dominates and leads to surface enrichment of A. The enrichment goes through a maximum at intermediate temperatures, and the curve shifts toward lower temperatures when the displacement rate is lower for the same reasons as outlined above for the depletion case.

3.2. Segregation with preferential interstitial-atom association

Thus far we have explored the effects of preferential defect migration via A-atoms without preferential defect-atom association in a highly concentrated solid-solution alloy. In order to describe systems such as Ni-Si where strong binding of the interstitials to the undersized atoms is likely to exist, we have performed model calculations for an A-B alloy with 5 at% A that include preferential interstitial associa-

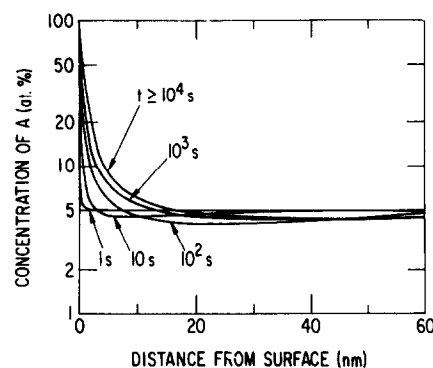


Fig. 4. Concentration of component A as a function of depth for several irradiation times. B-5 at% A alloy, foil thickness 500 nm, displacement rate 10^{-3} dpa/s, $H_{Av}^m = H_{Bv}^m = 1.28$ eV, $H_{Ai}^b = 1.0$ eV, $H_{Ai}^m = 0.9$ eV, $H_{Bi}^m = 0.15$ eV, temperature 500°C .

tion with A-atoms as described by eqs. (33) and (34). Using as a guideline the calculations of Dederichs et al. [9], we assumed a migration energy for the A-interstitial of $H_{Ai}^m = 0.9$ eV (corresponding to that of in-place rotation of a mixed dumbbell) in conjunction with a binding energy of $H_{Ai}^b = 1.0$ eV (corresponding to the conversion of a B-B dumbbell to a mixed A-B dumbbell), and a migration energy for the B-interstitial (assumed to migrate as a B-B dumbbell) of $H_{Bi}^m = 0.15$ eV. The vacancy migration energies for the two components were set equal; $H_{Av}^m = H_{Bv}^m = 1.28$ eV.

Fig. 4 shows the calculated concentration profiles in the near-surface region obtained for 500°C at several times. As expected from eq. (32) $\{d_{Av}/d_{Bv} - d_{Ai}/d_{Bi} = 1 - \exp[(H_{Ai}^b - H_{Ai}^m + H_{Bi}^m)/kT] < 0\}$, the surface quickly becomes strongly enriched in A. Steady state approached at $\sim 10^4$ s or ~ 10 dpa. For this temperature, which is close to the maximum segregation temperature, the surface concentration rises from 5 to 95 at% A whereas the depletion in the center of the foil is moderate (4.4 at% A). It should be pointed out, however, that the calculations were performed for a system with complete miscibility. In a system such as Ni-Si, the solubility limit for Si (≈ 10 at%) would have been reached after a short irradiation time, and precipitation of Ni_3Si would have led to a more significant depletion in the interior of the foil.

Steady-state concentration profiles calculated with

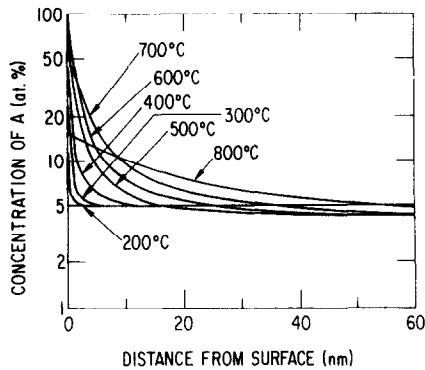


Fig. 5. Steady-state concentration of component A as a function of depth for several irradiation temperatures. Parameters are the same as for fig. 4.

the same physical parameters as those used in fig. 4 are shown for several temperatures in fig. 5. The profiles for the case of segregation due to preferential association of interstitials with one of the alloying elements, qualitatively resemble those observed for segregation due to preferential migration of defects via one of the components: At low temperatures, the concentration gradients are steep and extend only to shallow depths; with increasing temperature, they become less steep and penetrate farther into the foil.

Similarly, as in the cases of preferential defect migration, the amount of segregation as measured by

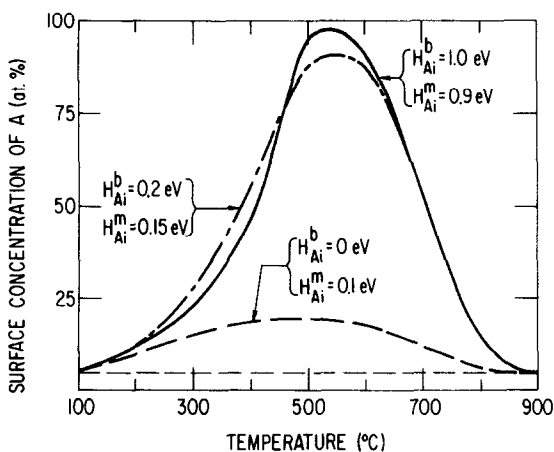


Fig. 6. Steady-state surface concentration of component A as a function of irradiation temperature. B-5 at% A alloy, foil thickness 500 nm, displacement rate 10^{-3} dpa/s, $H_{A_V}^m = H_{B_V}^m = 1.28$ eV, $H_{B_i}^m = 0.15$ eV. The curves are labeled to indicate the A-atom interstitial binding and migration energies.

the steady-state surface concentration goes through a maximum as shown in fig. 6. For comparison, results obtained with different interstitial-solute binding energies $H_{A_i}^b$ and A-interstitial migration energies $H_{A_i}^m$ are also shown in fig. 6. A smaller interstitial-A-atom binding energy and a correspondingly reduced migration energy ($H_{A_i}^b = 0.2$ eV, $H_{A_i}^m = 0.15$ eV) yields results similar to those of the previous case. A slightly preferential migration of interstitials via A-atoms ($H_{A_i}^b = 0$, $H_{A_i}^m = 0.1$ eV) with no binding causes appreciably less segregation. Qualitatively, these results are in accord with the corresponding magnitudes of the energy $H_{A_i}^b - H_{A_i}^m + H_{B_i}^m$ which determines the magnitude of the ratio d_{A_i}/d_{B_i} ; the energy values are 0.25, 0.2 and 0.05 eV, respectively. Details of the results, however, depend on the values of the individual energies and not only on this specific combination of energies.

The effect of displacement rate on segregation due to preferential interstitial association with A-atoms is illustrated in fig. 7. The peak in the steady-state surface concentration is shifted to a lower temperature as the displacement rate is decreased from 10^{-3} dpa/s, typical for charged-particle irradiations, to 10^{-6} dpa/s, corresponding to fast-reactor irradiations. In addition, both the temperature range in which severe segregation takes place and the magnitude of segrega-

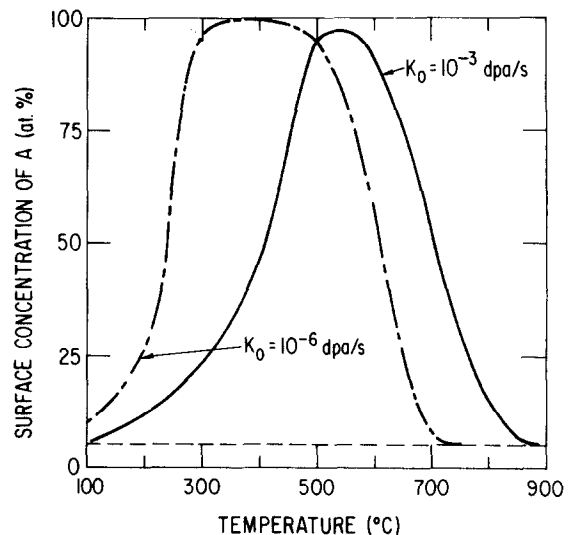


Fig. 7. Steady-state surface concentration of component A as a function of irradiation temperature for two displacement rates. Other parameters are the same as for fig. 4.

tion are larger at the lower displacement rate, according to the model calculations.

The results of the model calculations for concentrated alloys presented in this section exhibit segregation features qualitatively similar to those of the more extensive calculations which have been done previously using the Johnson–Lam model for dilute alloys: Segregation in concentrated alloys occurs in the same temperature regime as void swelling, and both show a maximum at approximately the same temperature. It may result from preferential migration of vacancies and/or interstitials via certain alloying elements as well as from preferential association of interstitials with an alloying element. Segregation becomes more severe and the temperature regime shifts to lower temperatures with lower dose rate.

4. Summary and conclusions

A simple model for radiation-induced segregation in concentrated binary alloys has been developed. The model describes the coupling between defect fluxes and alloying elements by partitioning the defect fluxes into fluxes occurring via A-atoms and via B-atoms and, similarly, partitioning the diffusion fluxes of the alloying elements into fluxes occurring via vacancies and via interstitials. The defect and atom fluxes can then be expressed in terms of concentrations and concentration gradients of all species present and a set of four diffusivity coefficients characteristics of distinct elementary diffusion events. In the simplest case, in which no preferential association between defects and A- or B-atoms occurs, the diffusivity coefficients contain only information about the local elementary diffusion event; e.g., d_{Av} includes the exchange frequency between an A-atom and a neighboring vacancy, and the jump distance. Preferential defect-atom association can be included in the model by appropriate modifications of the d 's. In order to keep the model simple, we have assumed random distributions of the alloying elements on a local scale, i.e., no clustering or ordering; have neglected correlation effects between subsequent jumps of the diffusing species; and have also neglected interstitialcy jumps simultaneously involving different atomic species. With these simplifications, the segregation problem can be cast into a set of three space-

and time-dependent coupled partial differential equations. This set can be solved numerically for representative geometries and appropriate initial and boundary conditions.

Model calculations have been performed for thin-foil geometry and binary solid solutions, assuming complete miscibility. The results are qualitatively similar to those obtained previously for dilute solutions using the Johnson–Lam model. The results show that segregation goes through a maximum as a function of temperature; this is similar to the temperature dependence of void swelling. Segregation can result from preferential migration of vacancies and/or interstitials via one alloying element or by preferential association of defects with one alloying element. An element A undergoes either depletion or enrichment, depending on whether the sign of the quantity $(d_{Av}/d_{Bv} - d_{Ai}/d_{Bi})$ is positive or negative, respectively. At steady state, the steepness of the concentration profile decreases and the depth of depletion or enrichment increases as the temperature increases. Maximum segregation occurs at lower temperatures, and the degree of segregation is more severe for lower displacement rates.

The model has been developed here only for binary alloys. The extension to alloys with more components is not expected to present any major difficulties. However, each additional alloying element introduces two additional diffusivity coefficients. Those coefficients that relate the exchange between an alloying element and vacancies can be estimated reasonably well, at least for some alloys, and can, in principle, be determined independently by thermal-diffusion and vacancy-concentration measurements. Our knowledge with regard to diffusivity coefficients involving interstitials is extremely restricted, and from a comparison of the model with experimental data on radiation-induced segregation, one can expect to obtain at best, rough values for these coefficients.

References

- [1] H. Wiedersich, P.R. Okamoto and N.Q. Lam, in: *Radiation Effects in Breeder Reactor Structural Materials*, Eds. M.L. Bleiberg and J.W. Bennett (AIME, New York, 1977) p. 801.
- [2] R.A. Johnson and N.Q. Lam, *J. Nucl. Mater.* 69 & 70 (1978) 424.

- [3] H. Wiedersich and P.R. Okamoto, in: *Interfacial Segregation*, Eds. W.C. Johnson and J.M. Blakely (ASM, Metals Park, 1978) p. 405.
- [4] P.R. Okamoto and L.E. Rehn, *J. Nucl. Mater.* 83 (1979) 2.
- [5] J.R. Manning, *Bull. Am. Phys. Soc.* 23 (1978) 287.
- [6] A.D. Marwick, *J. Phys. F: Metal Phys.* 8 (1978) 1849.
- [7] J.R. Manning, *Diffusion Kinetics for Atoms in Crystals* (Van Nostrand, Princeton, 1968).
- [8] A.D. LeClaire, *Physical Chemistry*, Vol. 10 (Academic Press, New York, 1970) p. 261.
- [9] P.D. Dederichs, C. Lehmann, H.R. Schober, A. Scholz and R. Zeller, *J. Nucl. Mater.* 69 & 70 (1978) 176.
- [10] A.C. Hindmarsh, Lawrence Livermore Laboratory Report UCID-30001 (1974).